ICAS Paper No. 80-2.1

TRANSONIC FIGHTER DESIGN USING
NUMERICAL OPTIMIZATION

by
P. V. Aidala
Grumman Aerospace Corporation
Bethpage, NY USA

The Twelfth Congress of the International Council of the Aeronautical Sciences

Munich, Germany
October 13-17, 1980

TRANSONIC FIGHTER DESIGN USING NUMERICAL OPTIMIZATION

P. V. Aidala
Grumman Aerospace Corporation
Bethpage, New York, U.S.A.

Abstract

A wing-body-canard transonic analysis code was developed and combined with numerical optimization. The combined code was applied to the design of an advanced fighter configuration. The configuration employs skewed-hinge variable camber geometry to provide appropriate wing section shapes and twist at transonic and supersonic flight conditions. The numerical optimization was applied to the design of the variable camber shapes to obtain transonic performance improvements. Two different models for the variable camber deflections were used in separate designs. Wind tunnel test results show good comparison with predictions. Only modest performance improvements were obtained. Numerical optimization is shown to be a useful tool in transonic fighter design where the analysis code can provide accurate performance information.

I. Introduction

Computational aerodynamic methods for the design of future configurations are becoming more important. New technology concepts and new configurational concepts are being developed to improve transonic performance. Accurate performance predictions are needed to confidently evaluate the benefits of new concepts. In addition, the pursuit of increased performance and reduced development time and costs intensify the use of three-dimensional computational analysis.

Significant strides have been made in the development of 3-D transonic aerodynamic design and analysis codes over the past five years. Although many of the methods are still in the evolutionary status, some have matured to the point that they can be applied to the solution of practical aircraft problems. However, application of these methods to real aircraft design problems has occurred only to a limited degree. The primary objective of the study reported here is to demonstrate that performance improvements and/or reduced development time and costs can be achieved by incorporating 3-D transonic methods into fighter aircraft design procedures. The basic approach used is to couple a 3-D transonic analysis code with numerical optimization. Numerical optimization was chosen because it provides the greatest flexibility of design problem definition and analysis code selection. A goal of this study is to develop a user-oriented, reliable, accurate design methodology of general applicability.

The work reported here was supported by the U. S. Air Force as the Advanced Transonic Technology study* and the Configuration Development of Advanced Fighters study.** Computer time for the results shown here was provided by NASA Ames Research Center on a CDC 7600. In addition, parts of the work were performed at NASA Ames through the Grumman-Ames Research Program Associate Program.

II. Design Problem Definition

The fighter configuration selected for the design methodology development need be capable of performing both current and future tactical mission requirements. Several studies of the interaction of mission requirements, technology advancements and weapon system configurations have shown the need for supersonic dash rather than today's transonic cruise, through enemy airspace. An objective of the Configuration Development of Advanced Fighters (CDAF) study was to derive, evaluate, analyze and test an advanced supersonic cruise fighter.

The "preferred concept" derived in the CDAF study is shown in Figure 1. The key performance requirements for the configuration are specified at supersonic cruise speeds greater than Mach 1.5 and at a transonic cruise and maneuver speed of Mach 0.9. Smooth skin, variable camber leading and trailing edge flaps are incorporated on the wing. The chord ratio of the leading edge device increases toward the tip, while that at the trailing edge device increases toward the root. This system enables simultaneous variations of wing camber and twist to produce efficient contours throughout the flight envelope.

The design of the baseline geometry (i.e., before any numerical optimization) began with linear supersonic and subsonic 3-D codes. The supersonic codes [1,2] were used to design the wing/canard camber, twist and thickness for minimum drag at supersonic cruise. The wing box geometry is then held fixed. (The canard geometry is held fixed, but with variable incidence available for trim.) The necessary wing device deflections for transonic cruise and maneuver were designed by using subsonic codes [3,4] and wind tunnel data of a similar variable

---

* Contract F33615-78-C-3014; AFWAL/FIMM
** Contract F33615-77-C-3045; AFWAL/FIMS

camber configuration. No aeroelastic changes to wing box twist were assumed. The final detailed camber shapes for transonic conditions were essentially determined with a "cut and try" approach.

With the wing box geometry dedicated to efficient supersonic cruise, the optimization technique of specifying a target pressure distribution does not provide a general method to determine the device deflections for best transonic performance. The transonic performance itself need be the criteria for determining the optimum design. The optimization problem for "best" transonic maneuver would be maximum trimmed lift, subject to a drag constraint (the available thrust). The capability to accurately and efficiently predict the transonic performance becomes crucial to the success of the numerical optimization. In general, the optimization problem for the "best" supersonic cruise fighter need consider the trade between more efficient transonic performance and more efficient supersonic cruise. This trade is evaluated through the take-off gross weight (TOGW) sensitivity for changes in transonic and supersonic performance of the particular configuration with its mission requirements. Consequently, it would be necessary to have accurate and efficient predictions of both transonic and supersonic performance for a successful design optimization.

It was the original intent of this study to investigate the trade between supersonic cruise and transonic maneuver performance. Two supersonic codes of Woodward [1,5] did poorly when evaluated with wind tunnel data on the baseline configuration. In addition, the configuration TOGW increase for a supersonic cruise drag increase was more than five times the TOGW decrease for a transonic maneuver drag decrease. A wing geometry change that results in a five count supersonic drag increase would need to produce more than a twenty-five count transonic maneuver drag decrease for no change in TOGW. The supersonic performance prediction uncertainty together with the TOGW sensitivity made a supersonic/transonic performance trade optimization impractical. The resulting design problem for numerical optimization was to determine the "best" variable camber deflections for transonic maneuver.

III. Analysis/Optimization Code

The need for wing-body-canard 3-D transonic analysis capability was identified very early in this study. The wing-body analysis code of Boppe (6) was selected as the base upon which to develop a wing-body-canard analysis code. The code uses line overrelaxation to solve a modified small disturbance equation in a "nested mesh" system. The nested mesh technique employed in the code was adapted in a straightforward manner to provide wing-body-canard analysis capability. Figure 2 illustrates the technique for a wing-body-canard combination. Other modifications to the code include global mesh adaptations for wing-canard planforms and provisions in the flow field solution to allow two lifting surfaces and their accompanying wakes. A more complete discussion of the code can be found in (7).

The code analysis capability was evaluated with wind tunnel data for the baseline configuration. Figure 3 shows results for three camber shapes. The variable camber deflections increase from the supersonic cruise (no deflections) through transonic cruise to transonic maneuver (greatest deflections). The code does not model the nacelles or vertical tail which are present in the data. (The drag contribution of the nacelles and vertical tail is estimated at twenty counts.) The computational mesh places fifteen analysis stations on the wing, eight analysis stations on the canard and eighty streamwise points on each airfoil section. A typical computation requires approximately ten minutes CPU time. A representative comparison of predicted and measured wing pressures is shown in Figure 4.

The wing-body-canard analysis code was coupled with the COPES and CONMIN routines of Vanderplaats. [8,9] The COPES code is a control program that connects the numerical optimization code CONMIN with the aerodynamic analysis code. The resulting computer code was named PANDORA - Preliminary Automated Numerical Design Of Realistic Aircraft. The structure of the PANDORA code allows the numerical optimization to be coupled to any analysis code. Several "analysis" codes could be used together to provide information for the optimization. This information might be supersonic performance, TOGW changes or mechanical system constraints. The available computer resources represent the only limit of complexity.

IV. Design Problem Numerical Modeling

The numerical optimization requires the choice of design variables and how they modify the configuration geometry. Two types of design functions are typical: piecewise airfoil section shape functions and complete wing section shape functions. Examples from 2-D applications can be found in (10) and (11). Two design approaches, corresponding to the two types of design functions mentioned above, were used in this study.

For the first approach, the design variables were a mathematical representation of the variable camber device geometry. The variable camber segmentation is shown in Figure 5. Figure 6 illustrates the equation relating a design variable V(N) to a device deflection $\Delta Z(N)$. The equations used represent the classical solution of a deflected, cantilevered beam. Small deflections are assumed, so that changes in the device surface area are ignored. This choice of design variables does not penalize the supersonic performance since the devices can return to the supersonic cruise shape. (There was no mechanical system limits imposed on the deflections.) Additional design variables can be incorporated by subdividing the variable camber segments.

Originally, eleven design variables were used to "deflect" the wing devices as sketched in Figure 7. A twelfth design variable was used to change the angle of attack. Later, sixteen design variables were used by subdividing four of the original camber segments. The four most outboard segments were subdivided first (segments 8-10 in Figure 7) and then, separately, the four most inboard segments were subdivided (segments 1-4 in Figure 7.) The starting wing geometry was the transonic maneuver shape of the baseline configuration.

The second approach used a set of design variables that was much simpler than the first. At each of the five defining span stations in Figure 7, two wing section shapes were specified and the optimization determined the best linear combination of the two shapes. The design variable at each span station represents the weighting factor for combining the two shapes, as shown in Figure 8. One of the sets of shapes used was the baseline transonic cruise wing sections. The other set of shapes was the transonic maneuver wing sections, but with reduced trailing edge deflections at the two most inboard stations. The sections have a common wing box shape, so that their combination results in geometry changes only where device deflection occurs.

The design variables of the first approach provide the capability to evaluate more complex camber shapes. The best mathematical representation of the variable camber devices is that which simulates the mechanical system being considered. Then, in principal, all possible wing section shapes that the mechanical system can provide are included in the "design space" the optimization process searches. The numerical optimization could be used to compare the best aerodynamics available for each of several mechanical systems. The minimum amount of complexity, weight or cost of the mechanical system necessary to perform the mission requirements can be determined. The baseline configuration did not define a mechanism for its variable camber system. The numerical model used for this study was considered representative of a simple, general, variable camber mechanical system.

The second set of design variables provides the advantage of simplicity. As the design variables vary, it is easier to visualize the corresponding wing geometry. The aerodynamics of the gradient information (i.e., the effect of design variable perturbations) obtained during the optimization process can be easily interpreted by the user. Thus the "aerodynamic systems" being considered by the designer are evaluated. With fewer design variables, the numerical optimization searches a smaller design space. This reduces the necessary computer time, but may restrict the design space to a region that does not include the "true" optimum. The user need choose wing section shapes that provide the optimization process a geometry that will meet the design requirements. The success of numerical optimization is always dependent on the aerodynamic perception of the user, especially as the number of design variables is reduced.

The starting geometry for the numerical optimization was the baseline transonic maneuver device deflections. At transonic maneuver conditions, wind tunnel data showed flow separation on the wing and canard that was well beyond the modeling capability of the code analysis. In order to have flow conditions that could be predicted with some degree of confidence, the optimization was started at an angle of attack below that for the actual maneuver point. The flow solution at six degrees angle of attack was chosen for the starting conditions.

A well-known drawback of numerical optimization in aerodynamic design is the computer time for the many aerodynamic analyses. The most accurate aerodynamic analysis would be a "converged" wing-body-canard solution, including viscous effects, for each geometry perturbation in the optimization search. The limits of computer resources for this study did not allow this. In order to reduce the computer time usage, the need for including the viscous effects and the canard influence during the wing design optimization were evaluated.

Analysis of the baseline configuration showed little benefit of including a boundary layer model in the design process. The boundary layer would alter the magnitude of forces and moments, but it would not significantly change the relative influence of geometry perturbations. The numerical optimization uses the relative effects of geometry perturbations to choose the "best" design. The most significant effect of the boundary layer during the design would be flow separation. A fixed boundary layer shape (i.e., equivalent inviscid starting geometry) would not show any separation changes. If the flow separation were significant, then the boundary layer model is inadequate.

Evaluation of the canard influence (with both data and analysis) showed the only region of significant influence to be the forward part of the inboard wing sections. This region does not have any leading edge devices. A "constant" canard wake could have been included in the analysis. This would provide the essence of the canard influence for a small increase in computer time. It was felt to be unnecessary for the design problem of this study. Trim drag considerations for the wing design could be included by constraints or pitching moment penalty formulas in the numerical optimization.

Thus, for the wing design optimization, the transonic analysis in PANDORA did not include the canard and did not include viscous effects. An additional change from the usual analysis in PANDORA was the use of a thinned mesh to further reduce computing times. The grid used placed twelve analysis stations on the exposed wing and fifty streamwise points

on each wing section. Thirty five flow solution iterations were used for the analysis of each geometry perturbation.

The starting flow solution was the thinned-mesh, inviscid wing-body analysis results for six degrees angle of attack and Mach 0.9. The usual numerical optimization problem was to reduce the drag, subject to the constraints of not decreasing the lift or pitching moment. Alternative optimization problems used were to minimize the square root of the drag, with lift and pitching moment constraints, and to maximize the lift, with moment and drag constraints.

V. Design Results

Initial results using the first approach with twelve design variables produced a calculated drag reduction of more than thirty counts (for the inviscid, thinned-grid analysis). This was obtained with two PANDORA runs, each with two optimization iterations. The second run was started with the design variable values from the end of the first run, but the optimization history was not saved for starting the second run. Total CPU time was less than two hours. The changes in spanwise distribution of lift and drag are shown in Figure 9. The design "moved" quickly to the lower limit of the tolerance on the lift constraint (i.e., the lift was slightly below the constraint value). The pitching moment constraint was inadvertently specified such that it was violated at the start of the optimization. The optimization results increased the pitching moment by more than .01 to satisfy the constraint. The constraint value was not changed since the less negative pitching moment would reduce trim drag and the numerical optimization was apparently not penalized significantly. The first two runs had several errors in the wing geometry modeling. The most significant error allowed geometry changes to propagate inboard of .308 semispan. This region is inboard of the end of the trailing edge devices (the outboard edge of the nacelle). Subsequent runs corrected this error.

The optimization runs with sixteen design variables (see Section IV) were started with the results of the first two runs. The extra design variables for the tip and root regions were run separately. Each run had two optimization iterations. No significant drag reductions were obtained. To evaluate if the design shapes were the optimum available with this approach, three additional runs were made with sixteen design variables (the extra design variables were used in the root region). Two of these runs redefined the optimization criteria. This changes the optimization search directions so that different regions of the design space are explored. One run sought to minimize the square root of the drag, while the other sought to maximize the lift, with a drag constraint of not more than the starting value. The starting geometry was the result of the first two runs, and the pitching moment constraint was the same as for all previous runs. No significant design variable changes occurred. Two optimization iterations were done for the lift maximization and one optimization iteration was done for the square root of drag minimization. It is interesting to note that the initial search direction for these two runs was the same within one percent. The initial search direction did differ significantly between these additional runs and the basic drag minimization run.

The third run perturbed the starting values of the design variables. The perturbation raised the trailing edge at the two most inboard span stations. The rest of device geometry was that at the end of the first two optimization runs. The drag was to be minimized with lift and moment constrained. The gradient information from previous runs was used to calculate starting values that would satisfy the constraints but increase the drag. In one optimization iteration the drag was reduced more than fifty counts, but the design variables that were manually changed at the start did not return to their previous "optimum" values. The resulting design variable values were used to start a run with two optimization iterations. No significant change occurred.

The final result of all the optimization runs with this approach was a predicted drag reduction of more than forty counts, ignoring any changes in lift and moment (approximately -.01 and +.01, respectively). Total CPU time for all the optimization runs was less than four hours. The trailing edge location of all three inboard devices was raised. The leading edge location at span stations 0.544 and 0.816 moved downward, while that of the theoretical tip moved upward. A "full-grid", wing-body viscous analysis at the nominal design conditions showed the lift to be seven percent less than the starting value. Matching the starting lift value, the estimated drag reduction was less than six counts. With the trim drag reduction due to less negative pitching moment, the total expected drag reduction was approximately fifteen counts.

The second optimization approach used significantly less computer time because of the fewer number of design variables. Two runs, each with three optimization iterations, reduced the predicted drag value by more than twenty counts. Again, the starting solution violated the pitching moment constraint and the lift was reduced to the lower limit of its constraint value. Essentially all of the drag reduction occurred during the first run. A third run to minimize the square root of the drag produced no significant changes in two optimization iterations. Total CPU time was less than two hours. Relative to the baseline transonic maneuver geometry, the predicted drag reduction for this approach was essentially the same as for the first approach (more than forty counts). Changes in lift and moment were also the same. The trailing edge location of the two most inboard devices was raised, while that of the third (span station .544) was lowered. The

leading edge was moved downward at all three span stations. Again, a "full-grid", viscous, wing-body analysis indicated a drag reduction of less than six counts at the starting value of lift. With the expected trim drag change, the total drag reduction was again approximately fifteen counts.

The two "optimum" device deflections moved in opposite directions at span stations .544 and 1.0. The predicted performance is the same, which may or may not be the "true" optimum. There is little doubt of the non-uniqueness of a configuration design problem. The design space must include the true optimum if it is to be found with numerical optimization. If several optimums exist, then several different design space restrictions or different starting solutions are needed to find the other optimums.

A drag reduction of fifteen counts is very small compared to the total drag at transonic maneuver conditions. In fact, a thirty count drag reduction was felt to be the minimum for a "significant" impact on the configuration. However, if the computational analysis can be used to confidently predict that a given wing geometry is near "optimum", then considerable design time and costs can be saved. Several CPU hours is a small expense compared to that of the design, fabrication, and test of an additional set of wing devices. As improvements in both computer and code capability continue to be made, numerical methods become more cost effective. For example, simple code changes made after the design optimization runs described above have reduced the CPU time requirements more than twenty percent. Further CPU time reductions are possible. If existing faster computers are considered, CPU time reductions of more than a factor of two would be easily obtainable. Such a reduction would allow more accurate analysis calculations (e.g., explicit viscous effects, greater density grids) and yet use considerably less CPU time than that reported here.

VI. Test Results

The two devices geometries designed with the PANDORA code were tested in the Arnold Engineering Development Center 16T Propulsion Wind Tunnel in April 1980. As part of the CDAF study, the baseline geometry was tested in April 1979 and an alternate transonic maneuver geometry was tested in November 1979. For all tests, the Reynolds number was 3.0 million per foot for subsonic Mach numbers. The fifteenth scale model had a mean aerodynamic chord of 11.3 inches, and was instrumented with a six component balance and ninety six pressure taps distributed on the wing and canard.

The alternate transonic maneuver devices were designed manually after evaluation of the first wind tunnel test data. The alternate maneuver devices represent device deflections that are between those of the transonic cruise and original transonic maneuver. The model parts for the alternate maneuver geometry were made from the original transonic maneuver model parts. Thus the baseline geometry used to start the optimization was not available for the test in April. The alternate transonic maneuvering geometry was tested with the PANDORA geometries to provide a test repeat reference.

Test results for wing-body configurations are compared to each other and code predictions in Figure 10. Code predictions are good. The predicted drag levels agree with the data within fifteen counts at the lower lift value and within twenty five counts at the higher lift value. The data show that the two PANDORA shapes have essentially the same performance as predicted by the optimization runs. No wing-body data are available for the baseline transonic maneuver geometry.

Data for wing-body-canard configurations are shown in Figure 11. The relative performance of the three tested configurations is the same as in Figure 10. Code predictions are within twenty counts of the data. Nacelle off data for the baseline maneuver configuration are not available. The nominal lift coefficient for the numerical optimization is C_L=0.5. Ignoring trim drag, the data for the full configurations show no drag reduction at the design lift. The pitching moment change was +.032 for both PANDORA shapes, relative to the baseline. The trim drag reductions are fifteen and thirteen counts for the first and second shapes respectively. The moment change is much greater than what was predicted. The resulting trim drag reductions, however, are very close to what was predicted. The sources of the errors in the pitching moment prediction are still being investigated.

The test results show that the numerical optimization can provide performance improvements within the limits of the analysis capability. This study was limited to one particular design application for a supersonic cruise transonic fighter. As discussed in previous sections, the final design problem for numerical optimization was a small part of the complete configuration design problem. Approximations made during the design problem numerical modeling (e.g., trim drag benefits, viscous effects) reduced the measured performance improvements from that predicted by the optimization runs. The benefits of numerical optimization can be expected to increase as the accuracy and completeness of the numerical simulation of the design problem increases.

VII Conclusions

The results reported here show both the benefits and hazards of numerical optimization for aerodynamic design. The numerical optimization will work best when both the flow field analysis and numerical model of the design problem are accurate. Although greater computer resources are generally needed for more complex and accurate analysis, the cost of numerical optimization would still be less than that of additional wind tunnel testing. As both computer and analysis code

capability increase, numerical optimization will take a greater role in aerodynamic design. For a variable camber wing geometry, evaluation of different mechanical systems is well suited for numerical optimization. The details of the mechanical system dictate the design variables and shape functions. This automatically restricts the optimization to the proper design space--the result of the optimization must be a shape the system can provide. Numerical optimization could be used to evaluate the resulting performance of mechanical systems with different complexity, cost or weight. The aerodynamic designer can best use numerical optimization by running two or three iterations for a variety of geometries and starting conditions. The numerical optimization will conduct a systematic parametric evaluation using the flowfield analysis as if it were a wind tunnel. The computer can be used to compare many different configurations over several days time at a small fraction of the time and cost that would be needed to conduct a wind tunnel test.

References

1. Woodward, F. A., et. al., "Analysis and Design of Supersonic Wing-Body Combinations, Including Flow Properties in the Near Field," NASA CR-73106, 1967

2. Harris, R. V., "An Analysis and Correllation of Aircraft Wave Drag" NASA TM X-947, 1964.

3. Boppe, C. W., "A Computer Program for Calculating Subsonic Aerodynamics of Complex Wing-Body Configurations (A User's Guide)," Grumman Aerodynamics Technical Data Report No. 393-73-1, October 1973.

4. Mason, W. H., "Computation of Minimum Trim Drag Attainable on Complex Configurations and the Associated Design Spanloads," Grumman Memorandum EG-ARDYN-78-44, May 1978.

5. Woodward, F. A., "An Improved Method for the Aerodynamic Analysis of Wing-Body-Tail Configurations in Subsonic and Supersonic Flow," NASA CR 2228, 1973.

6. Boppe, C. W., "Computational Transonic Flow About Realistic Aircraft Configurations," AIAA Paper 78-104, January, 1978.

7. Boppe, C. W., and Aidala, P. V., "Complex Configuration Analysis at Transonic Speeds," presented at AGARD meeting on Subsonic/Transonic Configuration Aerodynamics, May 1980.

8. Vanderplaats, G. N., "COPES-FORTRAN Control Program for Engineering Synthesis," to be published.

9. Vanderplaats, G. N., "CONMIN--A FORTRAN Program for Constrained Function Minimization," NASA TM X-62282, August, 1973.

10. Vanderplaats, G. N., Hicks, R. M. and Murmann, E. M., "Application of Numerical Optimization Techniques to Airfoil Design," NASA SP-347, Part II, 1975.

11. Vanderplaats, G. N. and Hicks, R. M., "Numerical Airfoil Optimization Using a Reduced Number of Design Coordinates," NASA TM X-73151, 1976.

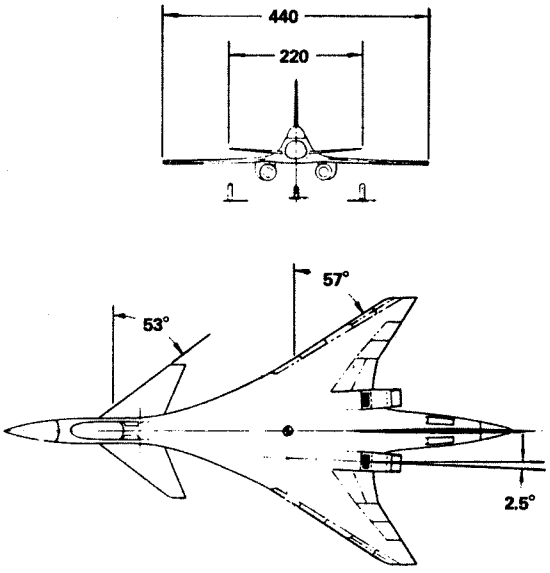

Figure 1. CDAF Preferred Concept.

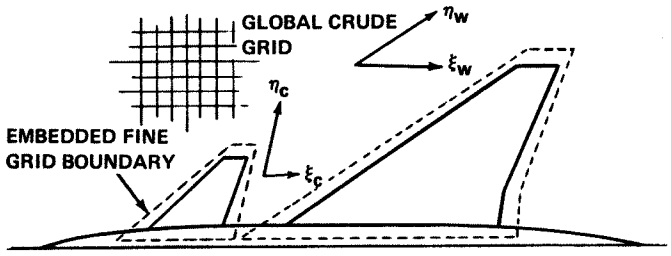

Figure 2. Embedded Grid System.

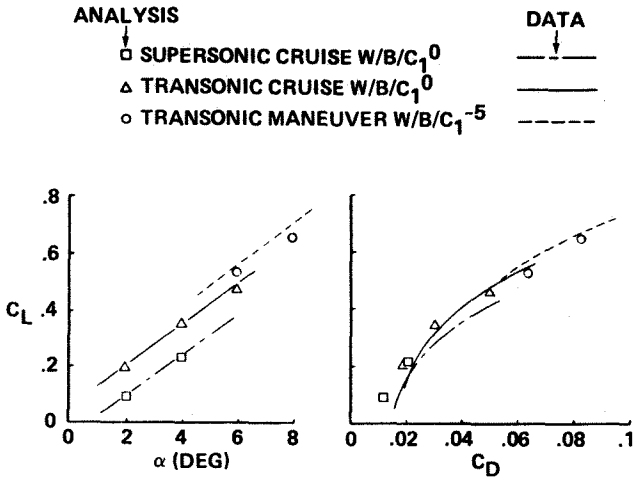

Figure 3. Wing-Body-Canard Force Predictions, Mach = 0.9.

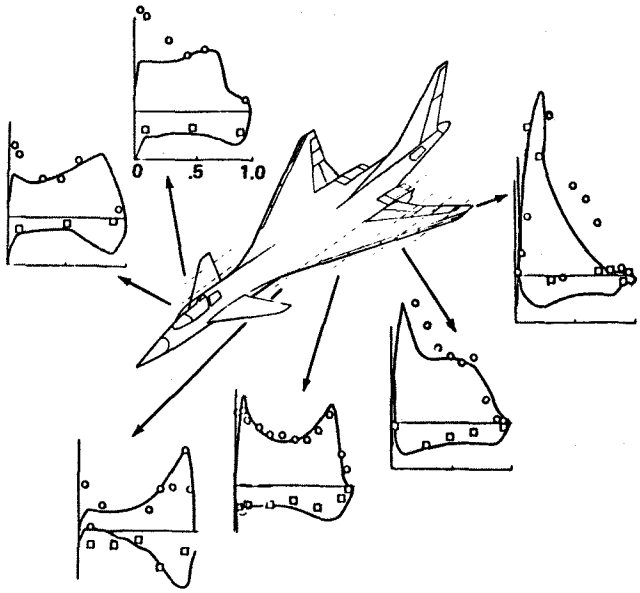

Figure 4. Wing-Body-Canard Pressure Distribution Prediction, Mach = 0.9 $C_L \sim 0.67$

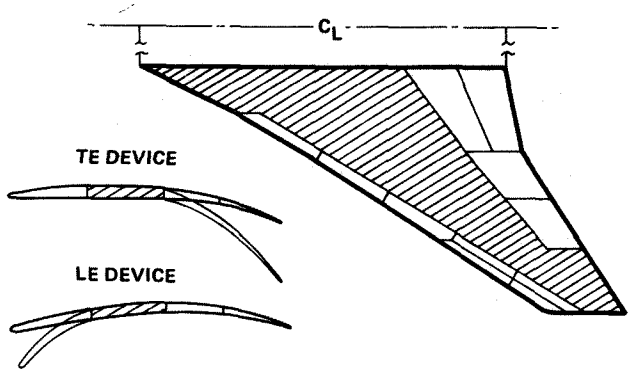

Figure 5. Variable Camber Segmentation.

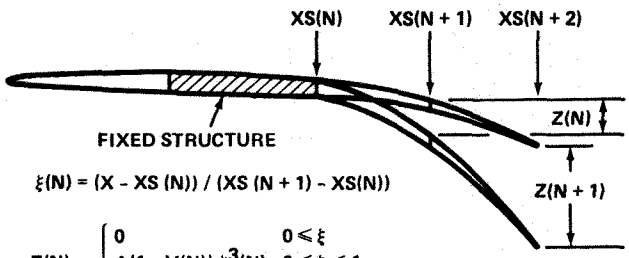

$$\xi(N) = (X - XS(N)) / (XS(N+1) - XS(N))$$

$$Z(N) = \begin{cases} 0 & 0 \leq \xi \\ A(1 - V(N))\,\xi^3(N) & 0 \leq \xi \leq 1 \\ B(1 - V(N))\,\xi\,(N) & 1 \leq \xi \end{cases}$$

WHERE

XS = CHORD STATION
Z = DEFLECTION
V = DESIGN VARIABLE
A,B = COEFFICIENTS FOR CONTOUR MATCHING

Figure 6. Variable Camber Deflection Model for Optimization.

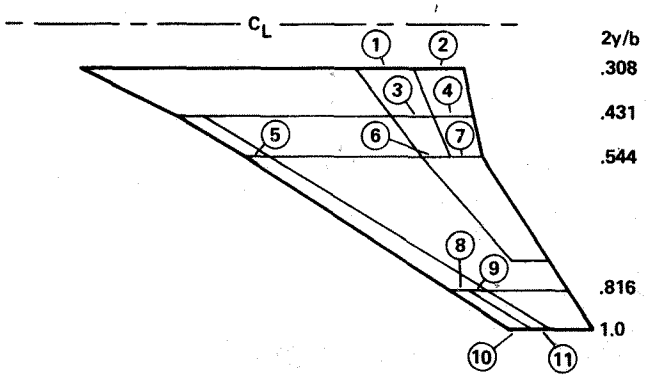

Figure 7. Deflection Model Design Variable Assignment.

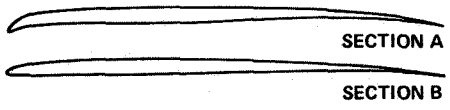

FOR WING SECTION N

$$Z(N) = ZA(N) \cdot (1 - V(N)) + ZB(N) \cdot V(N)$$

WHERE

Z(N) = WING SECTION ORDINATES AT SPAN STATION N
ZA(N) = WING SECTION A ORDINATES FOR SPAN STATION N
ZB(N) = WING SECTION B ORDINATES FOR SPAN STATION N
V(N) = DESIGN VARIABLE FOR SPAN STATION N

Figure 8. Variable Camber Shape Model for Optimization.

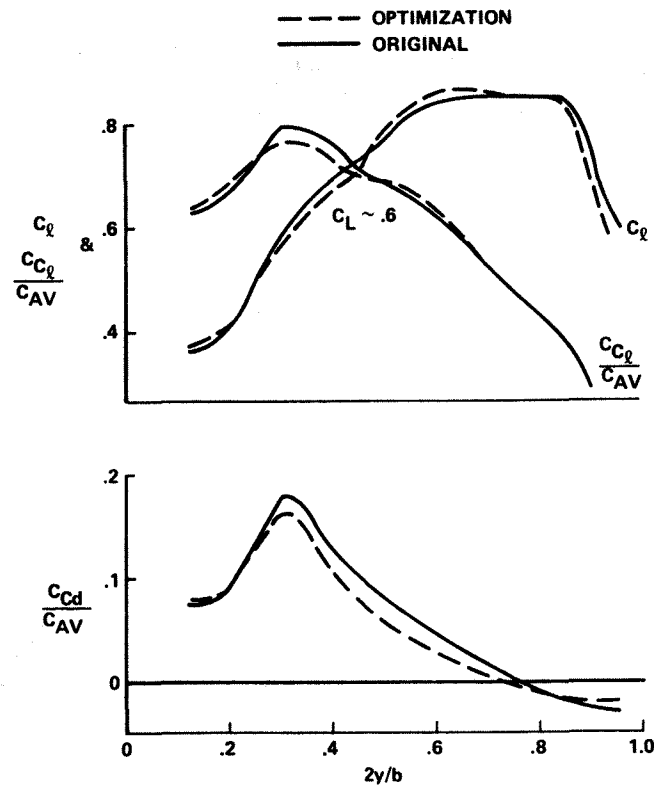

Figure 9. Initial Optimization Design.

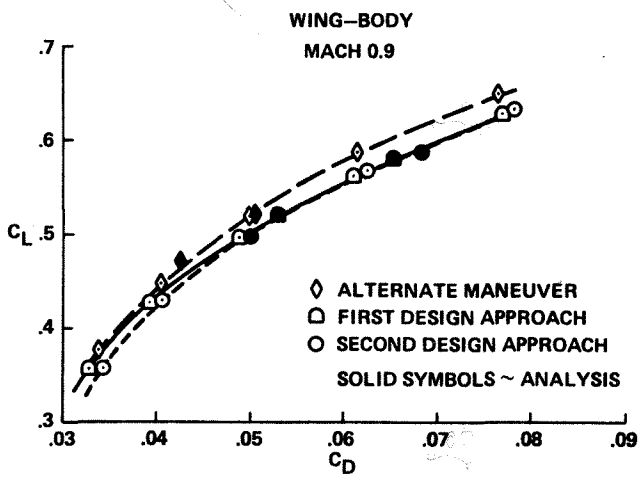

Figure 10. Wing-Body Test Results.

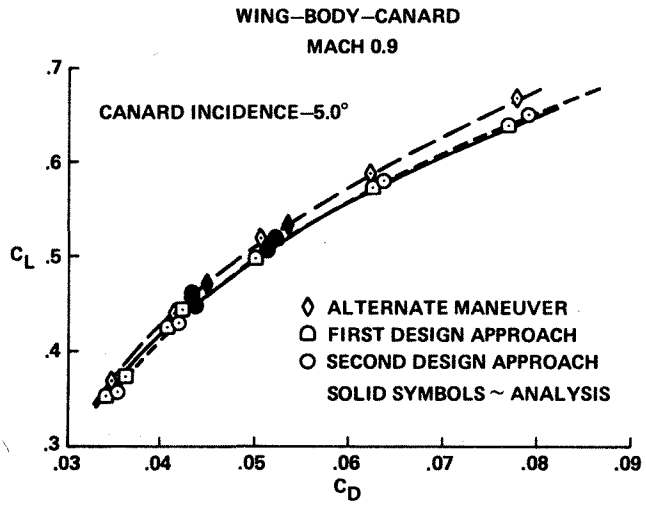

Figure 11. Wing-Body-Canard Test Results.